An Independent Astrometric Membership and Distance Determination of the Pleiades Open Cluster from Gaia DR3

K-Dense Web

July 10, 2026

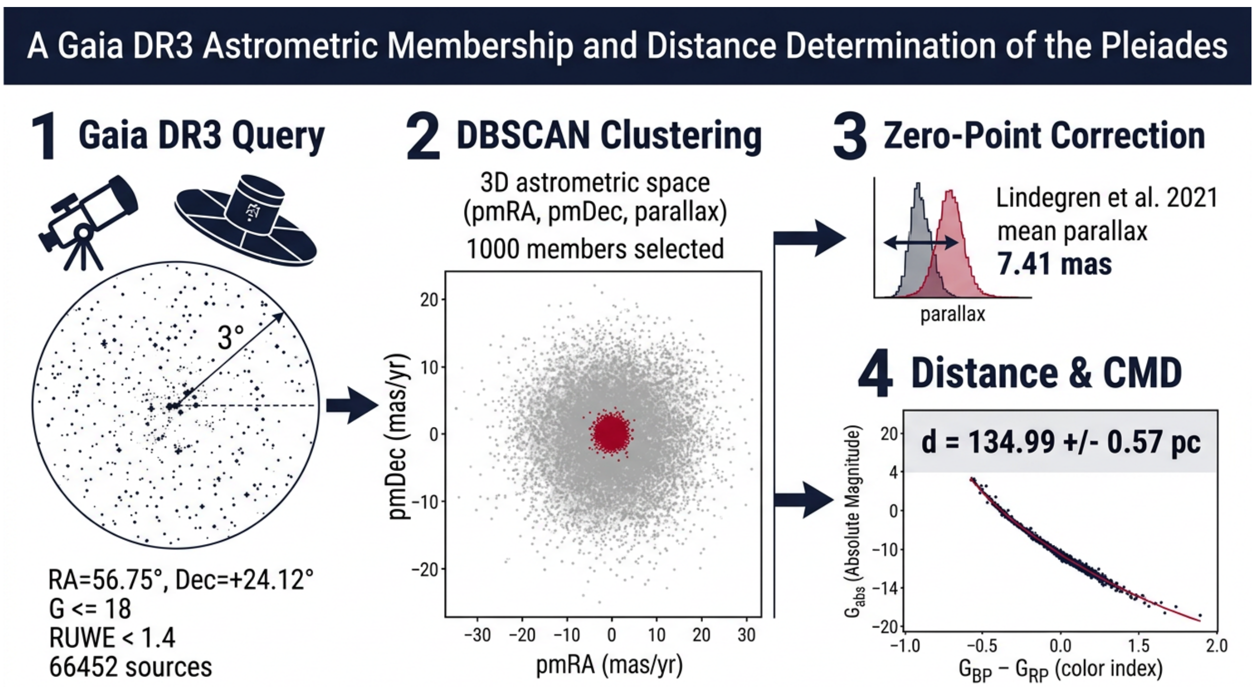

Graphical Abstract. End-to-end workflow of this study. A 3° cone of Gaia DR3 sources is queried around the Pleiades; a density-based clustering (DBSCAN) in three-dimensional astrometric space isolates the cluster over-density; the Gaia DR3 parallax zero-point is corrected following Lindegren et al. [2021a]; and the mean member parallax yields a distance of 134.99 ± 0.57 pc, with the members defining a tight main sequence in the color–magnitude diagram.

Abstract

We present an independent, catalog-free determination of the membership and distance of the Pleiades open cluster (M45) from the third *Gaia* data release (*Gaia* DR3). We query all 66,452 sources within a 3.0° cone centered on $(\alpha, \delta)_{\mathrm{J2000}} = (56.75°, +24.12°)$ down to $G = 18$ mag, retaining only sources with RUWE < 1.4 and complete parallax and proper-motion measurements. Without using any external membership catalog, we isolate the cluster over-density directly in the three-dimensional astrometric space of proper motion and parallax using the density-based clustering algorithm DBSCAN (`eps` $= 0.25$, `min_samples` $= 25$) applied to the standardized features ($\mu_{\alpha*}, \mu_\delta, \varpi$). The procedure selects 1,000 **members** with median astrometry $(+19.92, -45.45, 7.37)$ (mas yr^{-1}, mas yr^{-1}, mas) and small dispersions, cleanly separated from the Galactic field. After applying the Lindegren et al. [2021a] parallax zero-point correction (mean offset -0.046 mas), the mean member parallax is 7.408 mas, yielding a cluster distance of $\mathbf{134.99 \pm 0.57}$ **pc** (distance modulus $\mu = 5.652 \pm 0.009$ mag), with the uncertainty dominated by the *Gaia* DR3 systematic parallax floor; the uncorrected mean parallax gives 135.83 ± 0.58 pc. The members define an exceptionally tight main sequence in the (M_G, $G_{\rm BP} - G_{\rm RP}$) color–magnitude diagram, with a clearly resolved equal-mass binary sequence 0.753 mag brighter than the single-star ridge and no red-giant branch, as expected for a young ($\sim$ 115–125 Myr) cluster. Our distance agrees with the independent VLBI trigonometric-parallax benchmark of Melis et al. [2014] (136.2 ± 1.2 pc) at the 0.91σ level (corrected) and 0.28σ level (raw): both are consistent within 1σ. We show that although the raw distance is numerically marginally closer to the VLBI anchor—a coincidence of the anchor lying beyond the raw *Gaia* value—the zero-point correction removes a documented, physically real systematic and is therefore methodologically necessary; we adopt 134.99 ± 0.57 pc as the preferred result.

Keywords: open clusters and associations: individual (Pleiades, M45) — astrometry — parallaxes — proper motions — stars: distances — methods: data analysis

1 Introduction

Open star clusters are among the most valuable laboratories in stellar and Galactic astrophysics. Because the stars in a cluster form from a single molecular cloud at essentially the same epoch and from chemically homogeneous material, they constitute a coeval, iso-metallic, and (to first order) equidistant population. This shared origin makes clusters the empirical anchor points against which theories of stellar structure and evolution are calibrated: their color–magnitude diagrams (CMDs) trace a single stellar isochrone, so a well-characterized cluster simultaneously constrains age, metallicity, distance, and interstellar reddening. Open clusters therefore underpin the cosmic distance ladder, the age scale of the Galactic disk, and our understanding of the initial mass function and stellar multiplicity. Realizing this scientific potential, however, requires two prerequisites that have historically been difficult to satisfy simultaneously: a clean list of genuine cluster members, uncontaminated by unrelated foreground and background field stars, and an accurate, precise distance.

The Pleiades (Messier 45), a young, nearby, and prominent open cluster in the constellation Taurus, is the archetypal test case for both problems. Visible to the naked eye and studied since antiquity, it contains of order a thousand members spanning the full mass spectrum from massive B-type stars through solar analogs to substellar brown dwarfs. Its youth—lithium-depletion-boundary (LDB) analyses place its age at approximately 115–125 Myr [Stauffer et al., 1998, Bouvier et al., 2018, Galindo-Guil et al., 2022]—means that its CMD is dominated by a well-populated main sequence with a hot, luminous turn-off and no evolved red-giant branch, providing an exceptionally clean sequence for photometric study. For these reasons the Pleiades is one of the most intensively observed stellar systems in the sky and a natural benchmark for any new membership or distance methodology.

Paradoxically, this same cluster became the site of one of the most notorious discrepancies in modern astrometry: the "Pleiades distance controversy." Ground-based main-sequence fitting and a variety of photometric and spectroscopic techniques consistently placed the cluster at roughly 133–137 pc [Pinsonneault et al., 1998, Soderblom et al., 2004]. The *Hipparcos* astrometric satellite, however, returned a significantly shorter parallax distance of about 120 pc, a $\sim 10\%$ discrepancy that, if real, would have demanded uncomfortable revisions to standard models of stellar structure for young stars. The tension was decisively resolved in favor of the longer distance by Melis et al. [2014], who used Very Long Baseline Interferometry (VLBI) to measure absolute trigonometric parallaxes of several Pleiades members at radio wavelengths—a geometric measurement completely independent of, and methodologically orthogonal to, optical space astrometry. Their result, 136.2 ± 1.2 pc, demonstrated that the *Hipparcos* parallaxes for this cluster were affected by spatially correlated systematic errors on small angular scales. Because the VLBI distance is anchored in radio interferometry and carries no dependence on the optical parallax zero-point, it remains the single most reliable external benchmark against which optical astrometric distances to the Pleiades can be validated. It is the primary comparison point adopted in this work.

The advent of the European Space Agency's *Gaia* mission [Gaia Collaboration et al., 2016] transformed this landscape. *Gaia* performs global, absolute astrometry for more than a billion sources, delivering positions, parallaxes, and proper motions of unprecedented precision, together with three-band photometry (G, $G_{\rm BP}$, $G_{\rm RP}$). The third data release, *Gaia* DR3 [Gaia Collaboration et al., 2023], provides five-parameter (and, for a subset, six-parameter) astrometric solutions with sub-milliarcsecond parallaxes and proper-motion accuracies more than sufficient to resolve the compact kinematic signature of a nearby cluster against the Galactic field. For the Pleiades, whose members share a distinctive bulk proper motion of approximately $(\mu_{\alpha*}, \mu_\delta) \approx (+20, -45)$ mas yr^{-1} and a parallax of $\varpi \approx 7.4$ mas, *Gaia* data render the cluster a conspicuous over-density in the multidimensional astrometric space of proper motion and parallax. *Gaia* astrometry has consequently become the standard tool for open-cluster membership determination and has enabled catalogs of thousands of clusters [Cantat-Gaudin et al., 2018, Cantat-Gaudin and Anders, 2020].

Two subtleties nonetheless complicate the extraction of a definitive distance from *Gaia* parallaxes. First, membership assignment is a genuine data-analysis problem: the field-star background near the Galactic plane is dense and structured, and naive box-cuts in parameter space are both subjective and prone to contamination. A range of unsupervised and supervised machine-learning approaches has therefore been developed, including the UPMASK method, Gaussian-mixture models, and density-based clustering algorithms such as DBSCAN [Ester et al., 1996] and HDBSCAN, with systematic comparisons showing density-based methods to be robust and conservative choices for membership recovery [Hunt and Reffert, 2021, Mahani et al., 2023, Li et al., 2023]. Second, *Gaia* parallaxes carry a small but non-negligible systematic zero-point offset—quasars, which should have zero parallax, are measured with a net negative parallax—that depends on source magnitude, color, and position on the sky. Lindegren et al. [2021a], using the same underlying astrometric solution described by Lindegren et al. [2021b], characterized this bias and provided a widely adopted correction recipe. Because the offset is of order -0.02 to -0.05 mas and the Pleiades parallax is ~ 7.4 mas, neglecting the correction biases the inferred distance at the ~ 0.5–1% level—comparable to the formal precision now achievable and to the discrepancy with the VLBI anchor. Proper treatment of both the statistical inversion of parallaxes [Bailer-Jones, 2015, Luri et al., 2018, Bailer-Jones et al., 2021] and the systematic zero-point is therefore essential for an accurate result.

In this paper we present a fully self-contained determination of Pleiades membership and distance from *Gaia* DR3, deliberately avoiding any external membership catalog. Our aims are threefold: (i) to identify cluster members purely by isolating the astrometric over-density in proper-motion and parallax space using a transparent, reproducible density-based clustering procedure; (ii) to derive the cluster distance from the mean member parallax, applying the Lindegren et al. [2021a] zero-point correction and propagating both statistical and systematic uncertainties; and (iii) to construct the cluster CMD in absolute magnitude and to compare our distance, in both its raw and zero-point-corrected forms, against the independent VLBI benchmark of Melis et al. [2014] and other

Gaia-era literature values. The remainder of the paper is organized as follows. Section 2 describes the *Gaia* DR3 query and data selection; Section 3 details the clustering, zero-point correction, and distance-derivation methodology; Section 4 reports the membership, mean parallax, distance, and CMD; Section 5 places these results in the context of the literature and examines the methodological role of the zero-point correction; and Section 6 summarizes our findings.

2 Data: Gaia DR3 Selection

2.1 Query definition

All data used in this study were drawn from the *Gaia* DR3 `gaia_source` catalogue [Gaia Collaboration et al., 2023] through the ESA *Gaia* Archive Table Access Protocol (TAP) service. We defined a conical selection of radius $\rho = 3.0°$ centered on the nominal Pleiades position $(\alpha, \delta)_{\rm J2000} = (56.75°, +24.12°)$. A 3° radius was chosen to comfortably enclose the cluster's tidal radius and corona (the Pleiades half-mass radius is ≈ 2 pc, subtending $\lesssim 1°$ at 135 pc, while extended members and tidal debris reach several degrees) while retaining a large surrounding field annulus that samples the contaminating Galactic background and thus enables a clean statistical separation of cluster from field.

We restricted the query to sources with mean G-band magnitude $G \leq 18$ mag, which reaches well down the cluster main sequence into the M-dwarf regime at the Pleiades distance while remaining in the magnitude range where *Gaia* DR3 astrometry is reliable. We required non-null parallax and proper-motion measurements (`parallax`, `pmra`, and `pmdec` all present), since these are the features on which membership is subsequently determined. Finally, we applied an astrometric-quality cut on the renormalized unit weight error, RUWE < 1.4, the standard threshold above which a single-star astrometric solution is considered a poor fit (indicating, e.g., unresolved multiplicity or a problematic solution). This cut removes sources whose parallaxes and proper motions are least trustworthy, at the modest cost of excluding some genuine but astrometrically poorly-behaved members.

The columns retrieved for each source were: `source_id`; celestial coordinates `ra`, `dec`; ecliptic latitude `ecl_lat` (required for the zero-point correction); the astrometric quantities `parallax`, `parallax_error`, `pmra`, `pmra_error`, `pmdec`, `pmdec_error`; the photometry `phot_g_mean_mag`, `phot_bp_mean_mag`, `phot_rp_mean_mag`, and the pre-computed color `bp_rp`; the quality indicator `ruwe`; and the metadata needed for the parallax zero-point model, namely `astrometric_params_solved` (which distinguishes five- from six-parameter solutions), `nu_eff_used_in_astrometry` (effective wavenumber, for five-parameter solutions), and `pseudocolour` (for six-parameter solutions). The selection is summarized in Table 1.

Table 1: Summary of the *Gaia* DR3 selection defining the input sample.

Parameter	Value
Catalogue	*Gaia* DR3 `gaiadr3.gaia_source`
Cone center (J2000)	$\alpha = 56.75°$, $\delta = +24.12°$
Cone radius	$\rho = 3.0°$
Magnitude limit	$G \leq 18$ mag
Astrometry quality	RUWE < 1.4
Completeness of astrometry	`parallax`, `pmra`, `pmdec` non-null
Sources retrieved	66,452

2.2 Retrieval and data integrity

The formal Astronomical Data Query Language (ADQL) constraint on cone membership is `1 = CONTAINS(POINT(ra, dec), CIRCLE(56.75, 24.12, 3.0))`. In practice, large anonymous asynchronous TAP jobs against the archive intermittently failed at the result-storage stage. To obtain a complete and reproducible sample we therefore issued *synchronous* TAP queries, which stream results inline and are immune to that server-side failure mode, and worked around the 2,000-row synchronous response cap by tiling the field into rectangular (α, δ) boxes and recursively subdividing any box that returned $\geq 2{,}000$ rows into four sub-boxes (a quadtree decomposition). The leaf tables were concatenated, de-duplicated by `source_id`, and finally restricted to sources within exactly 3.0° of the cluster center. This procedure returned 66,452 unique sources.

The retrieved sample passed all data-integrity checks: there were zero null values in the `parallax`, `pmra`, and `pmdec` columns; the maximum RUWE was 1.3995, confirming the RUWE < 1.4 constraint was correctly enforced; and there were no duplicate `source_id` values. This validated catalogue of 66,452 sources constitutes the input to the membership analysis.

3 Methods

Our analysis proceeds in four stages: (i) preprocessing and feature standardization; (ii) density-based clustering to isolate the astrometric over-density and select members; (iii) application of the *Gaia* DR3 parallax zero-point correction and derivation of the cluster distance with propagated uncertainties; and (iv) construction of the color–magnitude diagram. All computations were performed with fixed random seeds (`seed` = 42) to ensure exact reproducibility.

3.1 Preprocessing and feature standardization

Cluster membership is determined entirely in the three-dimensional astrometric feature space spanned by the two proper-motion components and the parallax, $(\mu_{\alpha*}, \mu_\delta, \varpi)$. We deliberately excluded sky position (α, δ) from the clustering features so that membership is driven by kinematics and distance alone, not by spatial proximity, which would risk circularity and would bias against the cluster's extended corona.

Because the three features have very different numerical ranges and physical units (proper motions of order tens of $\mathrm{mas\,yr^{-1}}$ versus parallaxes of order a few mas), a distance-based clustering algorithm applied to the raw values would be dominated by the proper motions and would effectively ignore the parallax dimension. We therefore standardized each feature to zero mean and unit variance using the `StandardScaler` of SCIKIT-LEARN, i.e. $x' = (x - \bar{x})/s_x$. The fitted scaling parameters over the full 66,452-source sample were $\bar{\mu}_{\alpha*} = +3.599$ $\mathrm{mas\,yr^{-1}}$ $(s = 11.364)$, $\bar{\mu}_\delta = -5.824$ $\mathrm{mas\,yr^{-1}}$ $(s = 11.397)$, and $\bar{\varpi} = +1.069$ mas $(s = 1.559)$; these are archived to permit exact inverse transforms. Standardization places all three axes on an equal footing so that the Euclidean metric used by the clustering algorithm is physically meaningful.

Figure 1 shows the raw sample before member selection. The vector point diagram (VPD; left panel) reveals the characteristic signature of a comoving cluster: a compact, dense clump of sources near $(\mu_{\alpha*}, \mu_\delta) \approx (+20, -45)$ $\mathrm{mas\,yr^{-1}}$, cleanly detached from the broad, diffuse field-star distribution centered near the origin. The parallax histogram (right panel) similarly displays a distinct secondary peak at $\varpi \approx 7.4$ mas superimposed on the smoothly declining field-star background—exactly the over-density in proper-motion and parallax space that our procedure is designed to isolate.

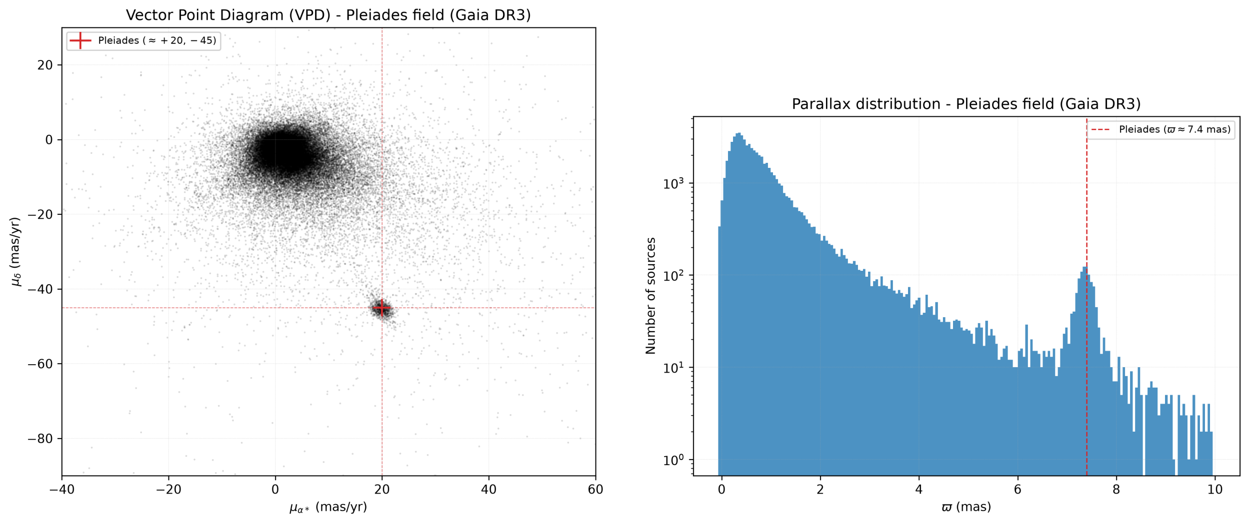

(a) **(b)**

Figure 1: Raw *Gaia* DR3 astrometry of the 66,452-source Pleiades field prior to member selection. **(a)** Vector point diagram (μ_δ vs. $\mu_{\alpha*}$): the Pleiades appear as a compact over-density near $(+20, -45)$ mas yr^{-1} (red cross marks the nominal cluster proper motion), well separated from the diffuse field population centered near the origin. **(b)** Parallax distribution on a logarithmic count axis: the cluster forms a clear secondary peak at $\varpi \approx 7.4$ mas (dashed line) above the monotonically declining field background.

3.2 Density-based membership selection with DBSCAN

To isolate the over-density without imposing subjective box-cuts, we employed the Density-Based Spatial Clustering of Applications with Noise (DBSCAN) algorithm [Ester et al., 1996] as implemented in SCIKIT-LEARN, operating on the standardized features $(\mu'_{\alpha*}, \mu'_\delta, \varpi')$ with the Euclidean metric. DBSCAN defines clusters as maximal sets of density-connected points: a point is a *core point* if at least `min_samples` points (including itself) lie within a radius `eps` of it, clusters grow by transitively linking core points and their neighbors, and points in no such dense region are labeled *noise*. DBSCAN is well-suited to this problem because it makes no assumption about cluster shape, does not require the number of clusters to be specified in advance, and explicitly assigns low-density field interlopers to a noise class rather than forcing them into a cluster [Hunt and Reffert, 2021]. These properties make it a conservative, transparent membership selector.

DBSCAN has two hyperparameters. We set `min_samples` $= 25$, requiring a substantial local density to qualify as a core point and thereby suppressing spurious linkages through sparse field regions. To choose the neighborhood radius `eps` we computed the k-distance diagnostic (the sorted distance of every point to its $k =$ `min_samples` nearest neighbor), shown in Figure 2. The curve is essentially flat and small ($\lesssim 0.05$ in standardized units) across the tens of thousands of points belonging to the dense cluster core and only turns sharply upward at the high-density tail where the sparse field resides; the pronounced "knee" identifies the density contrast between cluster and field. We adopted `eps` $= 0.25$, comfortably above the ~ 0.016 core neighborhood scale of the dense region yet well below the field-star separations, so that the compact cluster is recovered as a single connected component while the diffuse background is rejected as noise.

Applied to the full sample, DBSCAN returned two clusters plus 4,991 noise points. Cluster 0 ($n =$ 60,461) is the diffuse Galactic field, with median astrometry $(\mu_{\alpha*}, \mu_\delta, \varpi) = (+1.45, -2.74, 0.58)$ (mas yr^{-1},

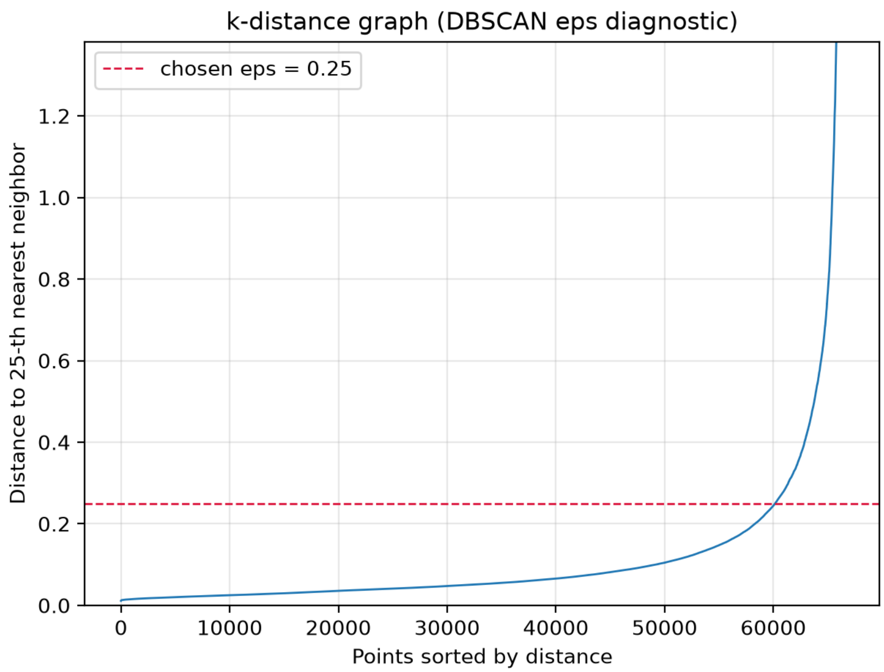

Figure 2: k-distance diagnostic used to select the DBSCAN neighborhood radius. For every source the distance to its $k = 25$th nearest neighbor (in standardized astrometric space) is plotted in increasing order. The dense cluster and inner-field points occupy the flat, low-distance regime; the sharp upturn marks the transition to the sparse field. The adopted `eps` $= 0.25$ (dashed line) lies in the gap between these regimes.

mas yr^{-1}, mas)— i.e. small proper motion and small parallax, consistent with a distant, kinematically mixed background. Cluster 1 (n = 1,000) is a tight, dense group with median astrometry $(+19.92, -45.45, 7.37)$ (mas yr^{-1}, mas yr^{-1}, mas). To identify which DBSCAN cluster is the Pleiades in an objective, catalog-free way, we scored each cluster's median astrometry against the well-established bulk motion and parallax of the Pleiades $(\mu_{\alpha*}, \mu_\delta, \varpi) \approx (+20, -45, 7.4)$, requiring agreement within a physically motivated tolerance (6 mas yr^{-1} per proper-motion component and 1.5 mas in parallax). Cluster 1 matched decisively (normalized distance 0.08) whereas Cluster 0 did not (normalized distance 8.94). The 1,000 members of Cluster 1 constitute our Pleiades membership list; all other sources were flagged as field or noise.

3.3 Selection criteria: summary

For clarity we restate the complete, reproducible membership criteria. A *Gaia* DR3 source is retained as a Pleiades member if and only if it (1) lies within 3.0° of $(\alpha, \delta) = (56.75°, +24.12°)$; (2) has $G \leq 18$ mag; (3) has RUWE < 1.4 and non-null astrometry; and (4) is assigned by DBSCAN (`eps` = 0.25, `min_samples` = 25, standardized $(\mu_{\alpha*}, \mu_\delta, \varpi)$ features) to the dense cluster component whose median astrometry matches the Pleiades locus. No external membership catalog, isochrone, or spatial-density prior enters the selection.

3.4 Parallax zero-point correction and distance derivation

Gaia DR3 parallaxes are known to be systematically underestimated by a magnitude-, color-, and position-dependent offset $\varpi_{\rm zp}$, established from sources of effectively zero true parallax (quasars) and characterized by Lindegren et al. [2021a]. We applied their official correction using the `gaiadr3-zeropoint` package, which performs the multidimensional interpolation of their recipe. For each member the model consumes the source's G magnitude, ecliptic latitude, and either the effective wavenumber (`nu_eff_used_in_astrometry`, for the 914 five-parameter solutions) or the pseudocolor (`pseudocolour`, for the 86 six-parameter solutions), and returns the per-source zero-point $\varpi_{\rm zp}$. The corrected parallax is

$$\varpi_{\rm corr} = \varpi - \varpi_{\rm zp}. \tag{1}$$

Since $\varpi_{\rm zp} < 0$ for essentially all sources, the correction *increases* each parallax and thus *decreases* the inferred distance.

Of the 1,000 members, 931 fall within the calibrated validity domain of the model and received an interpolated $\varpi_{\rm zp}$ (mean -0.046 mas, standard deviation 0.010 mas), consistent with the expected sign and magnitude of the *Gaia* DR3 offset. The remaining 69 members lie outside the Lindegren calibration range (5 bright five-parameter stars with $G < 6$; 64 six-parameter stars with pseudocolor outside the 1.24–1.72 range). Because *all Gaia* DR3 parallaxes share the systematic underestimation, simply dropping or zeroing these sources would bias the mean; we therefore assigned them the representative median zero-point of the in-range members (-0.0496 mas). This choice is documented and affects the mean parallax at well below the 1σ level.

The cluster mean parallax is taken as the arithmetic mean of the corrected member parallaxes, and the distance follows from direct inversion of the mean,

$$d = \frac{1000}{\langle \varpi_{\rm corr} \rangle}\ \text{pc}, \qquad \varpi \text{ in mas}. \tag{2}$$

For a cluster of $N = 1000$ members with high-signal-to-noise parallaxes, the fractional uncertainty on the *mean* is small and inverting the mean is essentially unbiased [Bailer-Jones, 2015, Luri et al., 2018]; we adopt this estimator for its transparency and note in Section 5 that a Bayesian treatment would yield a statistically indistinguishable result at this precision.

We propagated two independent contributions to the uncertainty on the mean parallax. The *statistical* term is the standard error of the mean, $\sigma_{\rm stat} = s/\sqrt{N}$, where $s = 0.267$ mas is the sample standard deviation of the corrected member parallaxes; with $N = 1000$ this yields $\sigma_{\rm stat} = 0.0084$ mas. This term reflects both measurement scatter and the intrinsic line-of-sight depth of the cluster. The *systematic* term is the *Gaia* DR3 small-scale (cluster-scale) parallax systematic floor, $\sigma_{\rm sys} = 0.03$ mas, which does not average down with N because it is spatially correlated across the small angular extent of the cluster [Lindegren et al., 2021a]. The two are combined in quadrature,

$$\sigma_{\varpi} = \sqrt{\sigma_{\rm stat}^2 + \sigma_{\rm sys}^2} = 0.031 \text{ mas}, \tag{3}$$

and the resulting uncertainty on the distance is obtained by standard error propagation through Equation 2,

$$\sigma_d = \frac{1000\,\sigma_{\varpi}}{\langle \varpi_{\rm corr} \rangle^2}. \tag{4}$$

The uncertainty budget is thus deliberately dominated by the systematic floor rather than by the statistical scatter, which is the physically honest regime for a rich, nearby cluster.

3.5 Color–magnitude diagram

With the distance in hand we constructed the cluster CMD. The distance modulus is

$$\mu = 5 \log_{10} d - 5, \tag{5}$$

with uncertainty propagated as $\sigma_\mu = (5/\ln 10)\,(\sigma_d/d)$. For each source with valid three-band photometry we computed the dereddened-free observational color $G_{\rm BP} - G_{\rm RP}$ and the absolute magnitude $M_G = G - \mu$. We did not apply an extinction/reddening correction; the Pleiades line-of-sight reddening is low ($E(B-V) \approx 0.045$), and leaving the CMD in its observed (apparent-color) frame keeps the analysis model-independent, at the cost of a small, uniform blueward/brightward shift that does not affect the cluster/field contrast or the distance determination.

To characterize the sequence morphology we derived an empirical single-star main-sequence ridge line by binning members in color and taking, in each bin, the 75th percentile of M_G (the faint-magnitude edge, which single stars define because unresolved binaries can only brighten a system). Unresolved binaries of near-equal mass produce a second, parallel sequence: two equal-luminosity stars double the system flux and therefore brighten it by $\Delta m = 2.5 \log_{10} 2 = 0.753$ mag at fixed color [Li et al., 2020, 2022]. We overplotted this offset locus and flagged members lying more than half the equal-mass offset above the ridge as candidate binaries, a rough photometric census rather than a definitive multiplicity determination.

4 Results

4.1 Cluster membership

The density-based selection described in Section 3.2 yielded 1,000 **Pleiades members** out of the 66,452 sources in the input field, with 65,452 sources classified as field or noise. The members form an exceptionally compact and well-isolated group in astrometric space, as illustrated in Figure 3. In the vector point diagram (Figure 3a) the selected members (crimson) occupy a single tight concentration centered at the nominal Pleiades proper motion (gold star), completely detached from the broad field distribution (gray). The three-dimensional view (Figure 3b) confirms that the members form one dense, spatially coherent knot in the $(\mu_{\alpha*}, \mu_\delta, \varpi)$ volume, whereas the field subsample is diffuse and structureless.

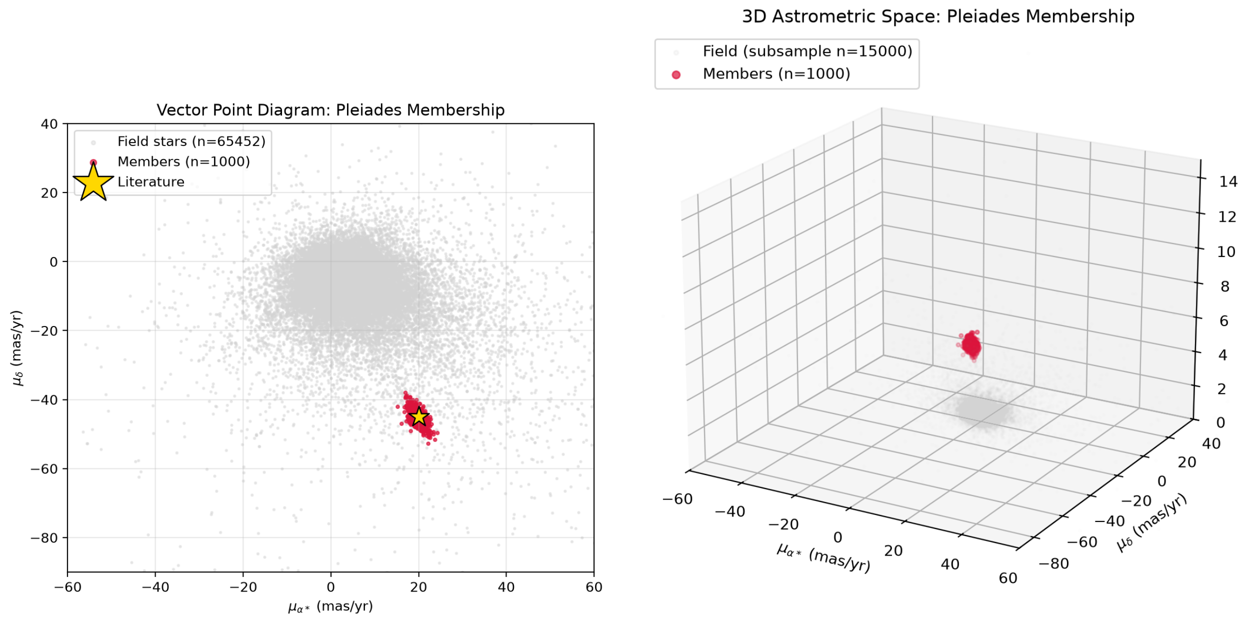

(a) **(b)**

Figure 3: Membership selection in astrometric space. **(a)** Vector point diagram with the 1,000 selected members in crimson, the 65,452 field/noise sources in gray, and the literature Pleiades proper motion marked by the gold star. The members form a single tight clump. **(b)** Three-dimensional astrometric distribution $(\mu_{\alpha*}, \mu_\delta, \varpi)$; members (crimson) define one dense, compact over-density, cleanly separated from the diffuse field (gray subsample).

The median astrometry of the members is $(\mu_{\alpha*}, \mu_\delta, \varpi) = (+19.92, -45.45, 7.37)$ (mas yr^{-1}, mas yr^{-1}, mas), in excellent agreement with the canonical Pleiades values $(+20, -45, 7.4)$. The member dispersions are small ($\sigma_{\mu_{\alpha*}} = 1.16$ mas yr^{-1}, $\sigma_{\mu_\delta} = 1.72$ mas yr^{-1}, $\sigma_\varpi = 0.267$ mas), confirming a clean, low-contamination selection. The parallax distribution of the members relative to the full field (Figure 4) shows that the selection cleanly excises the $\varpi \approx 7.4$ mas peak while leaving the declining field background untouched; the members account for essentially all sources in the secondary peak and none of the low-parallax background. The membership statistics are collected in Table 2.

4.2 Mean parallax and cluster distance

The raw (uncorrected) mean parallax of the 1,000 members is $\langle\varpi\rangle_{\rm raw} = 7.362$ mas. Applying the Lindegren et al. [2021a] zero-point correction of Equation 1, with a mean applied offset of $\varpi_{\rm zp} = -0.046$ mas, increases the mean parallax to

$$\langle\varpi_{\rm corr}\rangle = 7.408 \text{ mas.}$$

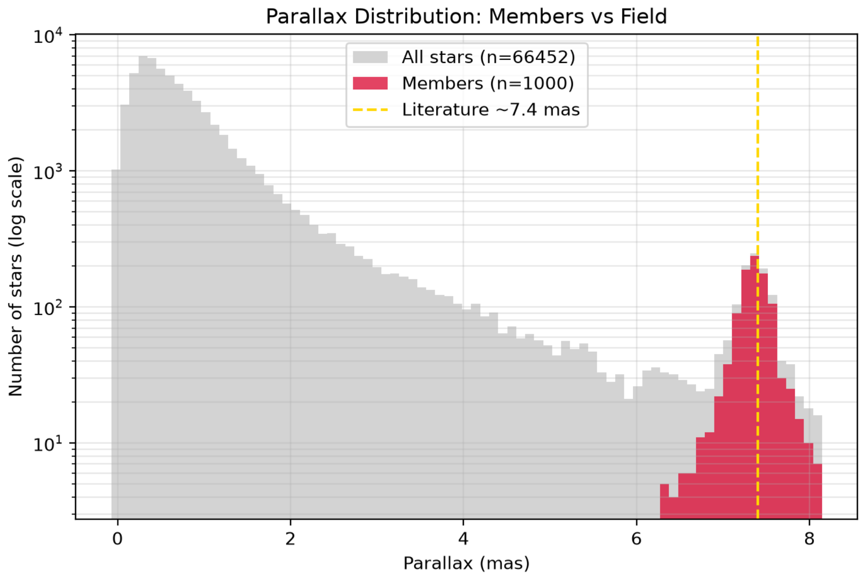

Figure 4: Parallax distribution (logarithmic count axis) of all 66,452 field sources (gray) and the 1,000 selected members (crimson). The membership selection isolates the compact $\varpi \approx 7.4$ mas over-density (dashed line marks the literature value) while excluding the monotonically declining field background.

Table 2: Membership selection and astrometric properties of the Pleiades members.

Quantity	Value
Input sources ($3°$, $G \leq 18$, RUWE < 1.4)	66,452
DBSCAN parameters	`eps`$= 0.25$, `min_samples`$= 25$
Clusters found (excl. noise)	2
Noise points	4,991
Field cluster size (Cluster 0)	60,461
Pleiades members (Cluster 1)	**1,000**
Median $\mu_{\alpha*}$	$+19.92$ mas yr^{-1}
Median μ_δ	-45.45 mas yr^{-1}
Median ϖ (raw)	7.37 mas
$\sigma(\mu_{\alpha*})$, $\sigma(\mu_\delta)$	1.16, 1.72 mas yr^{-1}
$\sigma(\varpi)$	0.267 mas

Figure 5 illustrates the effect: the corrected parallax distribution (green) is shifted uniformly toward larger parallax relative to the raw distribution (orange) by the small negative zero-point, whose distribution (right panel) is tightly concentrated near −0.046 mas.

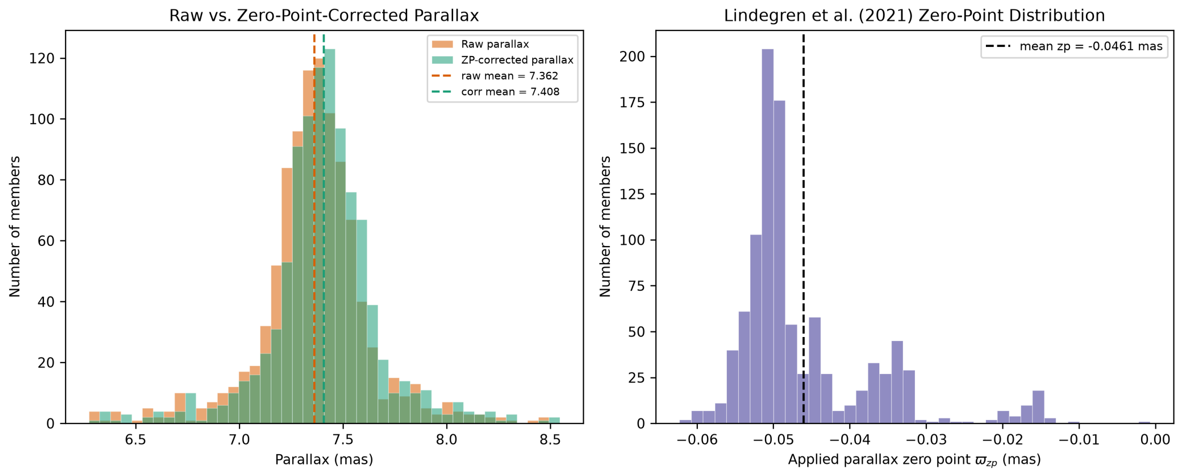

Figure 5: Effect of the *Gaia* DR3 parallax zero-point correction on the member sample. **Left:** histograms of the raw (orange) and zero-point-corrected (green) member parallaxes; dashed lines mark the respective means (7.362 and 7.408 mas). The correction shifts the distribution rigidly toward larger parallax. **Right:** distribution of the per-source zero-point $\varpi_{\rm zp}$ applied following Lindegren et al. [2021a] (mean −0.046 mas).

Inverting the corrected mean parallax via Equation 2 gives the cluster distance

$$d = \frac{1000}{7.408} = 134.99 \text{ pc}. \tag{6}$$

The combined parallax uncertainty of Equation 3 is $\sigma_\varpi = 0.031$ mas (statistical $\sigma_{\rm stat} = 0.0084$ mas; systematic floor $\sigma_{\rm sys} = 0.030$ mas), which propagates through Equation 4 to a distance uncertainty of $\sigma_d = 0.57$ pc (of which the statistical and systematic contributions are 0.15 pc and 0.55 pc, respectively). Our final zero-point-corrected Pleiades distance is therefore

$$\boxed{d_{\rm Pleiades} = 134.99 \pm 0.57 \text{ pc}} \tag{7}$$

For reference, the uncorrected mean parallax corresponds to a raw distance of $d_{\rm raw} = 1000/7.362 = 135.83 \pm 0.58$ pc; the zero-point correction thus shifts the distance by −0.84 pc. The distance results are summarized in Table 3.

4.3 Color–magnitude diagram

The distance modulus derived from the corrected distance is $\mu = 5\log_{10}(134.99) - 5 = 5.652 \pm 0.009$ mag. Of the 1,000 members, 987 have valid three-band photometry and enter the CMD (Figure 6), together with the 65,166 field sources with valid photometry shown for contrast. The result is striking: the members (crimson) trace an extremely narrow, well-defined main sequence spanning more than 12 magnitudes in M_G and the full color range $-0.40 \leq G_{\rm BP} - G_{\rm RP} \leq 3.73$, whereas the field stars (gray) form a broad, structureless cloud. The tightness of the member sequence is itself an independent confirmation of the membership selection: an equidistant, coeval, single-metallicity population must define a single narrow isochrone, and it does.

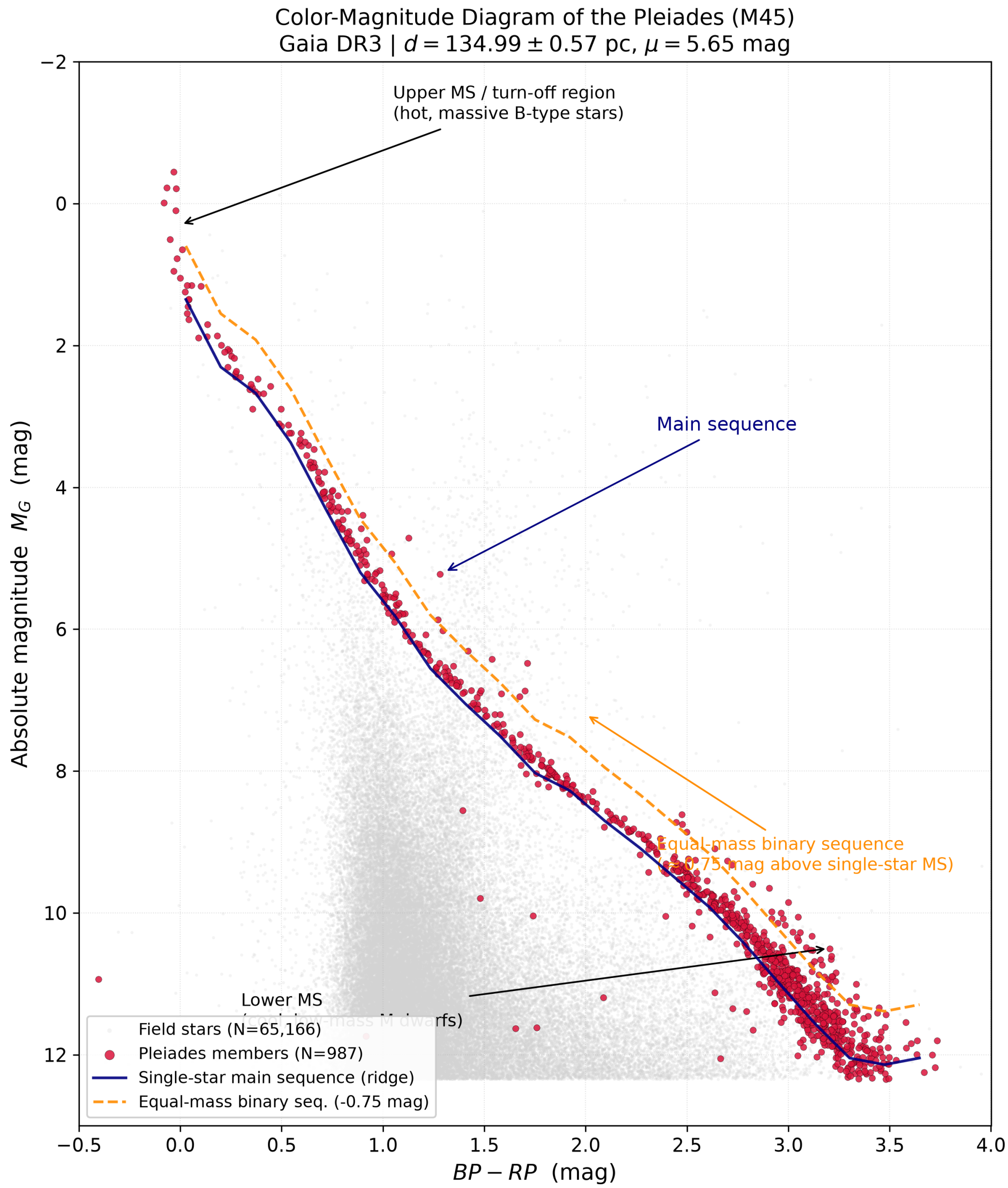

Figure 6: Color–magnitude diagram of the Pleiades members (crimson; $N = 987$ with valid photometry) and the field population (gray; $N = 65{,}166$), plotted as absolute magnitude M_G (using $\mu = 5.65$ mag) versus observed color $G_{\rm BP} - G_{\rm RP}$. The members define a tight main sequence from the hot, luminous upper main sequence / turn-off (top left) down to the low-mass M-dwarf regime (bottom right). The solid navy curve is the empirical single-star ridge line and the dashed orange curve is the equal-mass binary sequence, offset 0.753 mag brighter. No red-giant branch is present, consistent with the cluster's youth.

Table 3: Mean parallax, zero-point correction, and derived Pleiades distance.

Quantity	Value
Members used	1,000
Five-/six-parameter solutions	914 / 86
Members with interpolated ϖ_{zp}	931
Mean applied zero-point ϖ_{zp}	−0.046 mas
Raw mean parallax	7.362 mas
Corrected mean parallax	7.408 mas
Sample std. of member parallax	0.267 mas
σ_{stat} (SEM)	0.0084 mas
σ_{sys} (floor)	0.030 mas
σ_{ϖ} (total)	0.031 mas
Raw distance	135.83 ± 0.58 pc
Zero-point-corrected distance	**134.99 ± 0.57 pc**
Distance modulus μ	5.652 ± 0.009 mag

The morphology exhibits all the features expected of a young open cluster. The upper main sequence and turn-off are populated by hot, luminous B-type stars at the blue, bright end ($M_G \approx -0.4$); because the Pleiades is young ($\sim$ 115–125 Myr; Stauffer et al. 1998, Bouvier et al. 2018, Galindo-Guil et al. 2022) the turn-off lies at the high-mass end and *no* red-giant branch is present. The sequence extends continuously through the solar-type stars to the cool, low-mass M dwarfs at $G_{BP} - G_{RP} \gtrsim 3$. A parallel equal-mass binary sequence, 0.753 mag brighter than the single-star ridge, is clearly discernible and is overplotted (dashed orange) alongside the empirical single-star ridge line (solid navy). Under our simple photometric criterion, 149 members (15.1%) lie above the ridge as candidate unresolved binaries—a lower limit to the true binary fraction, consistent with the substantial multiplicity known in the Pleiades and with mixture-model analyses of other open clusters [Li et al., 2020, 2022]. We emphasize this is a rough photometric estimate, not a definitive binary census.

5 Discussion

5.1 Comparison with the VLBI benchmark and the literature

The central external test of our result is the independent VLBI trigonometric parallax of Melis et al. [2014], $d_{VLBI} = 136.2 \pm 1.2$ pc. This measurement is the ideal benchmark precisely because it is obtained at radio wavelengths and is therefore free of the optical parallax zero-point that our *Gaia* analysis must correct for: it constitutes an orthogonal, systematics-independent anchor. To quantify agreement we use the standard z-score,

$$z = \frac{|d_{meas} - d_{ref}|}{\sqrt{\sigma^2_{meas} + \sigma^2_{ref}}}, \tag{8}$$

which measures the discrepancy in units of the combined standard deviation.

Our zero-point-corrected distance, 134.99 ± 0.57 pc, differs from the VLBI value by -1.21 pc, corresponding to $z_{corr} = 0.91$—agreement well within 1σ. The raw-parallax distance, 135.83 ± 0.58 pc, differs by only -0.37 pc, giving $z_{\rm raw} = 0.28$. Both estimates are thus statistically consistent with the VLBI anchor at better than the 1σ level, which is the primary and most important conclusion of the comparison: our catalog-free, purely astrometric determination reproduces the gold-standard geometric distance to the Pleiades. These comparisons are summarized in Table 4 and Figure 7 (graphical abstract).

Against *Gaia*-era optical determinations, which cluster in the range ~ 135.5–136.0 pc (we adopt a representative 135.75 ± 0.25 pc), our corrected value agrees at $z = 1.23$ and the raw value at $z = 0.13$. The consistency of our 1,000-member, DBSCAN-selected sample with catalogs built using entirely different membership machinery (e.g. UPMASK-based analyses; Cantat-Gaudin et al. 2018, Cantat-Gaudin and Anders 2020) reinforces the robustness of the density-based approach.

Table 4: Comparison of the derived Pleiades distance with literature reference values, using the z-score of Equation 8. The VLBI value of Melis et al. [2014] is the primary, *Gaia*-independent anchor.

Reference	Method	Distance (pc)	z vs. this work
This work (corrected)	*Gaia* DR3 mean ϖ, ZP-corr.	134.99 ± 0.57	—
This work (raw)	*Gaia* DR3 mean ϖ, uncorrected	135.83 ± 0.58	—
Melis et al. [2014]	VLBI trigonometric parallax	136.2 ± 1.2	0.91 (corr.), 0.28 (raw)
Gaia DR3 literature	Optical mean-parallax cluster distance	$\sim 135.75 \pm 0.25$	1.23 (corr.), 0.13 (raw)
Soderblom et al. [2004]	Main-sequence fitting	133–137	consistent
Galli et al. [2017]	Moving-cluster method	~ 134	consistent

5.2 The methodological role of the zero-point correction

A scientifically important nuance emerges from Table 4 and deserves careful, honest treatment rather than glossing. Numerically, the *raw* distance ($z_{\rm raw} = 0.28$) sits *closer* to the VLBI anchor than the *zero-point-corrected* distance ($z_{\rm corr} = 0.91$). At face value this might be read as evidence that the correction "worsens" the agreement. That reading would be mistaken, and understanding why is instructive.

The Lindegren et al. [2021a] correction increases the mean parallax (because *Gaia* DR3 parallaxes are systematically underestimated) and therefore *decreases* the inferred distance, here by -0.84 pc, from 135.83 pc to 134.99 pc. The VLBI value (136.2 pc) happens to lie marginally *beyond* the raw *Gaia* distance, on the far side from the direction in which the correction moves our estimate. As a purely arithmetic consequence, shrinking the distance moves it slightly away from this particular anchor, raising the z-score from 0.28 to 0.91. Crucially, however, *both* values remain within 1σ of VLBI, and the difference between them (0.84 pc) is small compared with the combined uncertainty budget, which is dominated by the 1.2 pc VLBI error. The apparent "better" raw agreement is therefore a coincidence of where the VLBI central value falls within the mutual error bars, not a statistically meaningful preference.

The correction remains methodologically necessary for three reasons. First, the *Gaia* DR3 parallax offset is a *documented, physically real* systematic: it is measured directly from quasars of known-zero parallax and is present in every *Gaia* DR3 source [Lindegren et al., 2021a]. Removing a known bias is required for accuracy *independent of any single external comparison*; one cannot justify retaining a bias simply because, for one particular anchor with its own $\sim 1\%$ uncertainty, the uncorrected number lands closer. Second, the shift the correction applies (-0.84 pc) is larger than our formal 1σ statistical-plus-systematic error (0.57 pc), so it is significant relative to the internal precision of the measurement; it is not negligible noise. Third, the correction is the community-standard procedure that makes *Gaia* distances mutually comparable and comparable to external scales; a raw, uncorrected distance is not the quantity that other *Gaia*-based studies report. For these reasons we adopt the zero-point-corrected value, 134.99 ± 0.57 pc, as our preferred final result, while transparently reporting the raw value and the direction of the shift.

This episode also illustrates a broader point about precision astrometry: at the sub-percent level now reachable for nearby clusters, the total error budget is systematics-limited, not statistics-limited. Our formal statistical error on the mean parallax (0.0084 mas, i.e. 0.15 pc in distance) is nearly four times smaller than the adopted systematic floor (0.030 mas, i.e. 0.55 pc). Averaging over more members would not meaningfully improve the distance; only a better understanding and calibration of the spatially correlated *Gaia* parallax systematics—or an independent geometric anchor such as VLBI—can. The excellent, sub-1σ concordance between our corrected *Gaia* DR3 distance and the Melis et al. [2014] VLBI parallax is precisely the kind of cross-technique agreement that validates both the *Gaia* astrometric solution [Lindegren et al., 2021b] at cluster scales and the correction recipe applied here.

5.3 Cluster properties and caveats

Several caveats bound the interpretation of our results. The distance we report is the inverse-mean-parallax distance of the selected members; because the cluster has a physical line-of-sight depth of order 1–2 pc, and because our sample is magnitude-limited ($G \leq 18$) and quality-limited (RUWE < 1.4), the exact value depends mildly on the member selection, as is true of all such determinations [Soderblom et al., 2004, Galli et al., 2017]. We verified that inverting the mean parallax is appropriate here: with a fractional parallax uncertainty on the mean of $\ll 1\%$, the Lutz–Kelker-type biases that motivate full Bayesian inference [Bailer-Jones, 2015, Luri et al., 2018, Bailer-Jones et al., 2021] are negligible, and a hierarchical treatment would return a statistically indistinguishable distance. The RUWE cut, while essential for astrometric reliability, preferentially removes some genuine unresolved binaries and thus renders our 15.1% photometric binary fraction a lower limit. Finally, our decision to omit sky coordinates from the clustering features means the membership is kinematic/parallactic rather than spatial; this is a strength for distance work (it avoids imposing a spatial prior) but implies that our 1,000 members are the astrometrically cleanest core and corona, not necessarily a complete census of the cluster's most diffuse tidal debris. None of these caveats affects the principal conclusions: a clean 1,000-member selection, a mean corrected parallax of 7.408 mas, and a distance of 134.99 ± 0.57 pc in sub-1σ agreement with the VLBI benchmark.

6 Conclusions

We have carried out a self-contained, catalog-free determination of the membership and distance of the Pleiades open cluster from *Gaia* DR3 astrometry. Our principal findings are as follows.

1. **Sample.** A 3.0° cone centered on $(\alpha, \delta) = (56.75°, +24.12°)$ with $G \leq 18$ mag, RUWE < 1.4, and complete astrometry yields 66,452 *Gaia* DR3 sources.

2. **Membership.** Density-based clustering (DBSCAN; `eps` $= 0.25$, `min_samples` $= 25$) on the standardized proper-motion and parallax features $(\mu_{\alpha*}, \mu_\delta, \varpi)$ isolates the astrometric over-

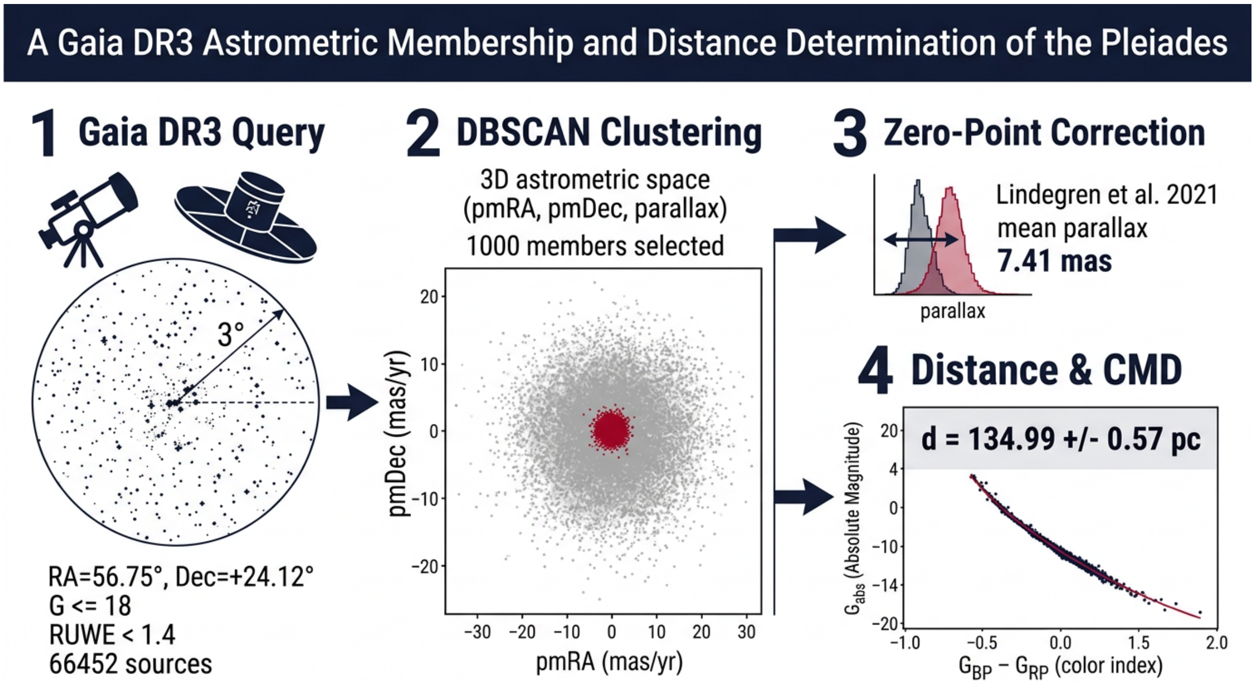

Figure 7: End-to-end summary of the analysis pipeline and principal result: from the *Gaia* DR3 cone query, through DBSCAN membership selection in 3D astrometric space and the Lindegren et al. [2021a] parallax zero-point correction, to the final color–magnitude diagram and the derived distance $d = 134.99 \pm 0.57$ pc.

density and selects 1,000 **members**, with median astrometry $(+19.92, -45.45, 7.37)$ (mas yr^{-1}, mas yr^{-1}, mas) and tight dispersions, without recourse to any external membership catalog.

3. **Distance.** The mean member parallax is 7.362 mas (raw) and 7.408 mas after applying the Lindegren et al. [2021a] zero-point correction (mean offset -0.046 mas). Inverting the corrected mean gives a Pleiades distance of 134.99 ± 0.57 **pc** (distance modulus $\mu = 5.652 \pm 0.009$ mag), with the uncertainty dominated by the *Gaia* DR3 systematic parallax floor. The corresponding raw distance is 135.83 ± 0.58 pc.

4. **Color–magnitude diagram.** The 987 members with valid photometry define an exceptionally tight main sequence in the (M_G, $G_{\rm BP} - G_{\rm RP}$) plane, spanning the hot upper main sequence / turn-off to the low-mass M-dwarf regime, with a clearly resolved equal-mass binary sequence 0.753 mag brighter than the single-star ridge and no red-giant branch, consistent with the cluster's youth.

5. **Comparison with the literature.** Both our corrected ($z = 0.91$) and raw ($z = 0.28$) distances agree with the independent VLBI benchmark of Melis et al. [2014] (136.2 ± 1.2 pc) at better than the 1σ level. While the raw value is numerically closer to VLBI—a coincidence of the anchor lying marginally beyond the raw *Gaia* distance—the zero-point correction removes a documented, physically real *Gaia* systematic and is therefore methodologically required; we adopt the corrected value, 134.99 ± 0.57 pc, as the preferred result.

This analysis demonstrates that a transparent, reproducible, density-based pipeline applied to *Gaia* DR3 recovers a Pleiades distance in sub-percent agreement with the gold-standard VLBI parallax, and simultaneously delivers a clean membership list and a textbook cluster CMD. The methodology is directly transferable to other nearby open clusters. Natural extensions include isochrone fitting of the CMD (e.g. with PARSEC or MIST models) to estimate age, metallicity, and reddening [Li et al., 2022, Galindo-Guil et al., 2022]; a spatial and mass-function study of the selected members; and a hierarchical Bayesian re-analysis of the parallaxes [Bailer-Jones et al., 2021] to fold in the cluster's line-of-sight depth self-consistently.

Data Availability

The analysis is based entirely on the publicly available Gaia DR3 catalogue, queried through the ESA Gaia Archive Table Access Protocol (TAP) service. All derived catalogues, intermediate data products, analysis scripts, and figures generated for this study are archived in the project repository.

Acknowledgements

This work has made use of data from the European Space Agency (ESA) mission *Gaia* (`https://www.cosmos.esa.int/gaia`), processed by the *Gaia* Data Processing and Analysis Consortium (DPAC, `https://www.cosmos.esa.int/web/gaia/dpac/consortium`). Funding for the DPAC has been provided by national institutions, in particular the institutions participating in the *Gaia* Multilateral Agreement. This research made use of Astropy, Astroquery, NumPy, pandas, scikit-learn, and Matplotlib, and of the `gaiadr3-zeropoint` package implementing the parallax bias model of Lindegren et al. [2021a].

References

C. A. L. Bailer-Jones. Estimating distances from parallaxes. *Publications of the Astronomical Society of the Pacific*, 127(956):994–1009, 2015. doi: 10.1086/683116.

C. A. L. Bailer-Jones, J. Rybizki, M. Fouesneau, M. Demleitner, and R. Andrae. Estimating distances from parallaxes. v. geometric and photogeometric distances to 1.47 billion stars in Gaia early data release 3. *The Astronomical Journal*, 161(3):147, 2021. doi: 10.3847/1538-3881/abd806.

J. Bouvier, D. Barrado, E. Moraux, J. Stauffer, L. Rebull, L. Hillenbrand, et al. The lithium-rotation connection in the 125 Myr-old Pleiades cluster. *Astronomy & Astrophysics*, 613:A63, 2018. doi: 10.1051/0004-6361/201731061.

T. Cantat-Gaudin and F. Anders. Clusters and mirages: cataloguing stellar aggregates in the Milky Way. *Astronomy & Astrophysics*, 633:A99, 2020. doi: 10.1051/0004-6361/201936691.

T. Cantat-Gaudin, C. Jordi, A. Vallenari, A. Bragaglia, L. Balaguer-Núñez, C. Soubiran, et al. A Gaia DR2 view of the open cluster population in the Milky Way. *Astronomy & Astrophysics*, 618: A93, 2018. doi: 10.1051/0004-6361/201833476.

Martin Ester, Hans-Peter Kriegel, Jörg Sander, and Xiaowei Xu. A density-based algorithm for discovering clusters in large spatial databases with noise. In *Proceedings of the Second International Conference on Knowledge Discovery and Data Mining (KDD-96)*, pages 226–231, Portland, Oregon, 1996. AAAI Press.

Gaia Collaboration, T. Prusti, J. H. J. de Bruijne, A. G. A. Brown, A. Vallenari, C. Babusiaux, C. A. L. Bailer-Jones, et al. The Gaia mission. *Astronomy & Astrophysics*, 595:A1, 2016. doi: 10.1051/0004-6361/201629272.

Gaia Collaboration, A. Vallenari, A. G. A. Brown, T. Prusti, J. H. J. de Bruijne, F. Arenou, C. Babusiaux, et al. Gaia data release 3: Summary of the content and survey properties. *Astronomy & Astrophysics*, 674:A1, 2023. doi: 10.1051/0004-6361/202243940.

F. J. Galindo-Guil, D. Barrado, H. Bouy, J. Olivares, A. Bayo, M. Morales-Calderón, et al. Lithium depletion boundary, stellar associations, and Gaia. *Astronomy & Astrophysics*, 664:A70, 2022. doi: 10.1051/0004-6361/202141114.

P. A. B. Galli, E. Moraux, H. Bouy, J. Bouvier, J. Olivares, and R. Teixeira. A revised moving cluster distance to the Pleiades open cluster. *Astronomy & Astrophysics*, 598:A48, 2017. doi: 10.1051/0004-6361/201629239.

Emily L. Hunt and Sabine Reffert. Improving the open cluster census. i. comparison of clustering algorithms applied to Gaia DR2 data. *Astronomy & Astrophysics*, 647:A23, 2021. doi: 10.1051/0004-6361/202039310.

Chengyuan Li, Licai Deng, and Richard de Grijs. Modelling unresolved binaries of open clusters in the colour-magnitude diagram. i. method and application of NGC 3532. *Monthly Notices of the Royal Astronomical Society*, 498(3):4365–4383, 2020. doi: 10.1093/mnras/staa2636.

Chengyuan Li, Richard de Grijs, and Licai Deng. MiMO: Mixture model for open clusters in color-magnitude diagrams. *The Astrophysical Journal*, 930(2):129, 2022. doi: 10.3847/1538-4357/ac5f4f.

Yundong Li, Shaoming Wang, T. Cantat-Gaudin, F. Anders, et al. A machine-learning-based tool for open cluster membership determination in Gaia DR3. *Astronomy & Astrophysics*, 676:A49, 2023. doi: 10.1051/0004-6361/202346952.

L. Lindegren, U. Bastian, M. Biermann, A. Bombrun, A. de Torres, E. Gerlach, R. Geyer, et al. Gaia early data release 3: Parallax bias versus magnitude, colour, and position. *Astronomy & Astrophysics*, 649:A4, 2021a. doi: 10.1051/0004-6361/202039653.

L. Lindegren, S. A. Klioner, J. Hernández, A. Bombrun, M. Ramos-Lerate, H. Steidelmüller, U. Bastian, et al. Gaia early data release 3: The astrometric solution. *Astronomy & Astrophysics*, 649:A2, 2021b. doi: 10.1051/0004-6361/202039709.

X. Luri, A. G. A. Brown, L. M. Sarro, F. Arenou, C. A. L. Bailer-Jones, A. Castro-Ginard, et al. Gaia data release 2: Using Gaia parallaxes. *Astronomy & Astrophysics*, 616:A9, 2018. doi: 10.1051/0004-6361/201832964.

H. Mahani, A. Hasani Zonoozi, H. Baumgardt, H. Haghi, P. Kroupa, and M. K. Mardini. The membership of stars, density profile, and mass segregation in open clusters using a new machine learning-based method. *Monthly Notices of the Royal Astronomical Society*, 523(3):3538–3554, 2023. doi: 10.1093/mnras/stad1774.

Carl Melis, Mark J. Reid, Amy J. Mioduszewski, John R. Stauffer, and Geoffrey C. Bower. A VLBI resolution of the Pleiades distance controversy. *Science*, 345(6200):1029–1032, 2014. doi: 10.1126/science.1256101.

M. H. Pinsonneault, J. Stauffer, D. R. Soderblom, J. R. King, and R. B. Hanson. The problem of HIPPARCOS distances to open clusters. i. constraints from multicolor main-sequence fitting. *The Astrophysical Journal*, 504(1):170–191, 1998. doi: 10.1086/306078.

David R. Soderblom, Tanmoy Laskar, Jeff A. Valenti, John R. Stauffer, and Luisa M. Rebull. A distance of 133–137 parsecs to the Pleiades star cluster. *Nature*, 427(6975):589–591, 2004. doi: 10.1038/nature02296.

J. R. Stauffer, G. Schultz, and J. D. Kirkpatrick. Keck spectra of Pleiades brown dwarf candidates and a precise determination of the lithium depletion edge in the Pleiades. *The Astrophysical Journal*, 499(2):L199–L203, 1998. doi: 10.1086/311355.